# Pitfalls in atmospheric correction of ocean color imagery: how should aerosol optical properties be computed?

Banghua Yan, Knut Stamnes, Wei Li, Bingquan Chen, Jakob J. Stamnes, and Si-Chee Tsay

Current methods for the atmospheric correction of ocean-color imagery rely on the computation of optical properties of a mixture of chemically different aerosol particles through combination of the mixture with it into an effective, single-particle component that has an average refractive index. However, a multicomponent approach in which each particle type independently grows and changes its refractive index with increasing humidity is more realistic. Computations based on Mie theory and radiative transfer are used to show that the two approaches result in top-of-the-atmosphere radiances that differ more than the water-leaving radiance. Thus, proper atmospheric correction requires a multicomponent approach for the computation of realistic aerosol optical properties. © 2002 Optical Society of America

*OCIS codes:* 010.1110, 010.1290, 010.4450, 290.0290.

## 1. Introduction

The wavelength dependence of the water-leaving radiance just above the ocean surface is usually referred to as the ocean color. Ocean color is the result of scattering and absorption by chlorophyll pigments as well as dissolved and particulate matter in the subsurface ocean waters. Thus the ocean color provides information on the concentrations of phytoplankton, dissolved organic matter, and particles in the water column. This implies that, at least in principle, these concentrations can be retrieved from measurements of the ocean color from space, on regional as well as global scales. However, the water-leaving radiance due to scattering and absorption in the ocean can be as low as a few percent of the top-of-the-atmosphere (TOA) radiance.[1] Consequently, it becomes very important to quantify and accurately remove the contribution from atmospheric molecules and aerosols to the TOA radiance. This removal is commonly referred to as atmospheric correction.

The Sea-viewing Wide Field-of-view Sensor (SeaWiFS) was designed to measure TOA radiances in eight bands between 412 and 865 nm. In ocean optics it is customary to distinguish between two basic types of water depending on their optical properties. In case 1 waters phytoplankton species and their derivative products (organic detritus and dissolved yellow colored matter, arising from zooplankton grazing, or natural decay of the algal cells) play a dominant role in determining the optical properties of the ocean. In case 2 waters a dominant contribution to the optical properties comes from resuspended sediments from the continental shelf, or from particles and/or colored dissolved organic matter in river runoff or urban/industrial discharge.[2] An algorithm for atmospheric correction of the SeaWiFS imagery obtained over case 1 waters was developed by Gordon and co-workers.[3,4] This algorithm utilizes 12 candidate aerosol models for nonabsorbing or weakly absorbing aerosols in the atmospheric-correction process. To study the atmospheric correction for strongly absorbing aerosols, Gordon and others considered four additional aerosols models.[4–6] The optical properties of aerosols vary in time and space. For atmospheric-correction purposes it is important to select candidate aerosol

B. Yan is with the Geophysical Institute, University of Alaska, Fairbanks, Fairbanks, Alaska 99775-7320. K. Stamnes (kstamnes@stevens-tech.edu), W. Li, and B. Chen are with the Department of Physics and Engineering Physics, Stevens Institute of Technology, Hoboken, New Jersey 07030. J. J. Stamnes is with the Department of Physics, University of Bergen, N-5007 Bergen, Norway. S.-C. Tsay is with the National Aeronautics and Space Administration, Goddard Space Flight Center, Greenbelt, Maryland 20771.

Received 9 April 2001; revised manuscript received 20 August 2001.

0003-6935/02/030412-12$15.00/0

models that span the range of conditions that one expects to encounter over the considered region. Schwindling *et al.*[7] measured direct atmospheric transmittance and sky radiance in La Jolla, California, to verify if the aerosol models selected by Gordon and co-workers[3–5] for SeaWiFS are adequate for ocean-color remote sensing from space. These researchers found that these aerosol models allow one to fit, within measurement inaccuracies, the derived values of the Angstrom coefficient and the pseudo phase function (the product of the single-scattering albedo and the phase function). However, additional measurements taken under different atmospheric conditions would be required to make a more general assessment of the suitability of these candidate aerosol models for atmospheric-correction purposes.

These 16 candidate aerosol models consist of several types of particles, each having its own characteristic chemical composition, size distribution and hygroscopicity.[8] The following questions then arise: How do we compute the optical properties of such a multi-component mixture of dry aerosol particles? And can we predict how these optical properties change with an increase in the humidity of the air in which the particles are suspended? The changes in the optical properties depend on how the particles grow and mix when they are exposed to humidity. Mixing is usually treated superficially in aerosol models, owing to lack of observational data, but the absorption by the aerosols will depend on how one treats a mixture of particles with different refractive indices and different hygroscopicities. Assuming a purely internally mixed aerosol population, one obtains optical properties that are different from those arising from assuming a purely externally mixed aerosol population.[9,10] As the relative humidity (RH) increases, water vapor condenses out of the atmosphere onto the suspended aerosol particles. This condensed water increases the size of an aerosol particle and changes its composition (and hence its refractive index). As a result its optical properties are correspondingly modified.[8,11,12]

The aerosol models used for atmospheric correction in the SeaWiFS operational algorithm are based on those constructed by Shettle and Fenn.[8] These models were based on the aerosol data available at that time, and they were designed to cover a wide range of atmospheric conditions. To save computational resources (since computers were much less powerful in the 1970s than they are today), Shettle and Fenn[8] decided to combine the different aerosol species into an effective single-component model (internal mixing) by averaging the refractive indices of the multicomponent aerosol mixture. This approach, which we shall refer to as the single-component (SC) approach, seemed to be a reasonable choice at the time. In view of the sparsity of observational data this SC approach has been used by the atmospheric community for a variety of purposes. To account for the change in optical properties with changing relative humidity Shettle and Fenn[8] used the SC approach to compute and tabulate the change in particle size and refractive index as a function of relative humidity. These tables provided a convenient set of optical properties that have been used extensively for a variety of purposes. In particular, these tables have been used in conjunction with Mie computations to obtain aerosol optical properties which are then used as a basis for atmospheric correction of ocean-color imagery.[3–6,13,14]

A more realistic approach would be to treat each aerosol component separately (external mixing), and compute its change in size and refractive index with relative humidity. The optical properties of a multicomponent mixture would be obtained first through the computation of the optical properties of each component and then the retrieval of the optical properties of the mixture as the concentration-weighted average of the optical properties of each aerosol component.[15] For convenience we refer to this procedure as the multicomponent (MC) approach. d'Almeida *et al.*[16] also discussed the MC approach: Each component is characterized by a specific log-normal distribution and a wavelength-dependent refractive index, and these two quantities then enable one to compute the optical properties of each component. Finally, the addition of the component properties, weighted by their respective mixing ratios, yields the optical properties of the aerosol type in question.[16] Here we should point out that although the MC approach is an advancement over the SC approach, it does not consider the effect of water uptake or the size distribution (and therefore optical properties) of different particle types mixing as they are emitted and transported away from source regions. Single-particle x-ray analysis and mass spectrometry methods have shown that particles rarely are composed of a single chemical component (see e.g., the results by Murphy *et al.*[17]). Rather they are mixtures of soluble (e.g., sea salt and sulfate) and insoluble (e.g., soot and dust) species. As components of different solubility are combined, the water uptake of the mixed particle changes. In addition, the size distribution of an existing aerosol can be changed by the condensation of gas phase species (e.g., $SO_2$ and organics) onto it.

Remote sensing of ocean color from space is a very difficult undertaking, owing to the small contribution of the water-leaving radiance (transmitted through the atmosphere) to the total TOA radiance. An error of a few percent in the TOA reflectance in the near-infrared (NIR) bands caused by the violation of the NIR black-pixel assumption will lead to a non-negligible error in the retrieval of ocean color.[18,19] Therefore accurate computation of the optical properties of the candidate aerosol models adopted for atmospheric-correction purposes becomes a matter of considerable importance. In this paper, we use an iterative scheme that is the most stable and economical scheme suggested by Shettle and Fenn[8] to compute the change in size and refractive index of individual aerosol components with increasing relative humidity, as well as an accurate Mie computa-

Table 1. Mode Radius $r_i$ ($i$ = 1 or 2) Defined in Eq. (1) for the Tropospheric and Urban Aerosol Models as a Function of Relative Humidity

| | Tropospheric Aerosol Model | Urban Aerosol Model | |
|---|---|---|---|
| RH | $r_1$ (μm) | $r_1$ (μm) | $r_2$ (μm) |
| 50% | 0.02748 | 0.02563 | 0.4113 |
| 70% | 0.02846 | 0.02911 | 0.4777 |
| 90% | 0.03884 | 0.04187 | 0.7061 |
| 99% | 0.05215 | 0.06847 | 1.4858 |

tional code to compute the optical properties of a multicomponent aerosol mixture.[15] A comprehensive radiative transfer code[20] properly modified to apply to the coupled atmosphere-ocean system[21,22] is employed to compute the TOA radiance in the eight SeaWiFS bands, and to assess the difference incurred through use of optical properties generated by the SC approach as compared with the more realistic MC approach.

### 2. Comparisons between Aerosol Optical Properties Computed Using the SC and MC Approaches

The 16 aerosol models employed as candidate models in the SeaWiFS algorithm for atmospheric correction of ocean-color imagery, include the Coastal, Maritime, Tropospheric, and Urban models introduced by Shettle and Fenn.[8] Each of these are used with relative humidities (RHs) of 50, 70, 90, and 99%, respectively, yielding a total of 16 different models. Except for the Tropospheric case, these aerosol models consist of two log-normal size distributions (LNDs) as follows[8]:

$$n(r) = \frac{\mathrm{d}N(r)}{\mathrm{d}r} = \sum_{i=1}^{2} \left[ \frac{N_i}{\ln(10) r \sigma_i \sqrt{2\pi}} \right] \times \exp\left[ -\frac{(\log r - \log r_i)^2}{2\sigma^2} \right], \quad (1)$$

where $N(r)$ is the cumulative number density of particles with radius $r$, σ is the standard deviation, and $N_i$ is the number density of particles with mode radius $r_i$. Here $r_i$ and σ depend upon the aerosol model and RH.[8] This distribution function represents the multi-modal nature of atmospheric aerosols that has been discussed in various studies.[23–27] Harris and McCormick[28] suggested the use of the sum of four LNDs, and Davies[29] used the sum of as many as seven LNDs to fit a measured aerosol size distribution. However, Whitby and Cantrell[30] showed that two modes are generally adequate to characterize the gross features of most aerosol distributions. Values of $r_i$ for the two modes ($i$ = 1,2) are given in Table 1 in Subsection 3.A.

#### A. Physical Differences between the Single-Component and Multicomponent Approaches

It is well known that the aerosol size and refractive index will change in a moist environment because water in the air condenses onto the aerosol. The growth in particle size due to the condensation of water vapor is described by[11]

$$r(a_w) = r_0 \left[ 1 + \rho \frac{m_w(a_w)}{m_0} \right]^{1/3}, \quad (2)$$

where the water activity $a_w$ of a soluble aerosol at radius $r$ [μm] can be expressed as

$$a_w = \mathrm{RH} \exp\left[ \frac{-2\sigma V_w}{R_w T} \frac{1}{r(a_w)} \right]. \quad (3)$$

Here $r_0$ is the dry particle radius, ρ is the particle density relative to that of water, $m_w(a_w)$ is the mass of condensed water, $m_0$ is the dry particle mass, RH is the relative humidity, σ is the surface tension on the wet surface, $V_w$ is the specific volume of water, $R_w$ is the gas constant for water vapor, and T is the absolute temperature [$K$]. Since the water activity changes not only the physical size of the aerosol but also its effective index of refraction, the relationship between water uptake [$m_w(a_w)/m_0$] and water activity for aerosols is of paramount importance. Considerable effort has been expended in this field over the past three decades.[11] Several of the parameters in Eqs. (2) and (3) depend on the aerosol chemical composition (particle density, mass of condensed water, surface tension), and these factors will be affected by the mixing of chemical components into and within the particles. This mixing is not accounted for by the MC approach.

The refractive index for the wet aerosol particle modified by the increased size is simply the volume-weighted average of the refractive indices of the dry aerosol substance ($n_0$) and the water ($n_w$) as follows

$$n = n_w + (n_0 - n_w) \left[ \frac{r_0}{r(a_w)} \right]^3. \quad (4)$$

From these formulas we note that (i) the magnitude of the particle growth and the change of refractive index with increasing RH depends on the size $r_0$ of the dry aerosol. The aerosol size in each of the 16 aerosol models spans a large range depending on the aerosol component. For example, the typical size range of dry soot particles lies between 0.005 and 20.0 μm.[16] This implies that the rate of change of size and refractive index due to increased RH will depend on the aerosol size, i.e., it is not a constant across the aerosol size range. (ii) The magnitude of the particle growth and the change of refractive index with increasing RH depends on the aerosol type because the water uptake [the ratio $m_w(a_w)/m_0$ in Eq. (2)] depends on the aerosol type.[11,31,32] The aerosol models introduced by Shettle and Fenn[8] consist of five groups: water solu-

ble (e.g., ammonium, organic compounds, etc.), dust-like (e.g., clay, quartz, etc.), soot (e.g., graphite, elemental carbon, etc.), sea salt (e.g., sodium, potassium chloride, etc.), and liquid water. Since the physical size of the aerosol may grow either because it is soluble or because it consists of an insoluble core with a soluble material coating, the rate of growth for a specific particle size differ from one aerosol component to another. As mentioned above other factors influencing particle growth, such as particle density and surface tension, are not accounted for in the MC approach.

Both the SC and MC approaches consider the particle growth and the change in refractive index of the aerosol due to increased RH as described by Eqs. (2)–(4). However, as mentioned above, the SC approach is based upon an effective refractive index obtained as an average over the multi-component aerosol population. This homogeneous mixing results in a single-component aerosol population that is assumed to adequately represent the actual multi-component mixture. This single-component aerosol population with an effective refractive index is then modified by the RH according to Eqs. (2)–(4). The resulting particle growth and change in refractive index are provided in Tables 4 and 5 of Shettle and Fenn.[8] The SC approach ignores the fact that different aerosol components grow and thereby change their refractive indices at different rates as the humidity increases. In contrast to the SC approach, the MC approach allows each aerosol component to grow and change their refractive indices independently with RH according to Eqs. (2)–(4). This heterogeneous mixing allows the size and refractive index of each component to be modified by the changing RH at all different aerosol sizes within the size distribution, and the optical properties of each aerosol component is computed separately for each modified particle size consistent with its modified refractive index.[15] Thus, the MC approach describes the particle growth and its change in refractive index caused by the increased RH for each particular size of the aerosol distribution, and for each component. However, this approach assumes that mixing of chemical components, which is known to occur[17,33,34] does not affect their hygroscopic growth, which is generally not the case.

The size and the real part of the refractive index affect the asymmetry factor $g$ (the first moment of the phase function) of the aerosol population, and the imaginary part of the refractive index affects its single-scattering albedo (SSALB), which is the ratio of the scattering to the extinction coefficient. From this discussion it is easy to understand that for a given aerosol size the SC approach will lead to a refractive-index distribution that is different from that produced by the MC approach. Conversely, for a given refractive index the SC approach will lead to a size distribution that is different from that produced by the MC approach.

### B. Comparisons between Aerosol Optical Properties Computed by the SC and MC Approaches

The difference between the SC and MC approaches in the way each particle is allowed to grow and change its refractive index with increasing RH, leads to significant differences in the resulting optical properties for a collection of aerosols consisting of more than one type of particles. As explained above, "type" here refers to the refractive index of the particle (i.e., its chemical composition) and its solubility or water uptake capacity (i.e., its hygroscopicity). Thus it is no surprise that these two approaches lead to different bulk optical properties (e.g., angular-scattering pattern or phase function and wavelength dependence of the optical depth) for the collection of particles. This difference arises because the bulk optical properties are obtained by averaging over optical properties of individual particles as determined by their sizes and refractive indices. Furthermore, if any of the particle types in the mixture are absorbing, then the SC and MC approaches will result in significant differences in the SSALB even for a dry mixture of particles. Also, the two approaches will give a different evolution of the SSALB as the particles grow owing to increasing RH. To quantify these effects we show results generated with the SC and MC approaches for the SSALB, the asymmetry factor $g$, and the wavelength dependence of the optical depth. But to save space, we present results only for the Tropospheric and Urban aerosols models at wavelengths of 443 and 865 nm. Similar results (not shown here) are obtained at other wavelengths and for the other candidate aerosol models. The Tropospheric aerosol model consists of weakly absorbing particles with a 70% water-soluble substance and a 30% dust-like substance. The Urban aerosol model consists of a mixture of weakly absorbing as well as absorbing particles with a 56% water-soluble substance, a 24% dust-like substance, and a 20% soot-like substance.

Figure 1 shows comparisons of the SSALB, the asymmetry factor ($g$), and the spectral dependence of the optical depth for the Tropospheric aerosol model computed with the two different approaches. As shown in Figs. 1(a) and 1(b), the SSALB depends weakly upon whether the SC or MC approach is adopted. This is understandable in view of the weak absorption. However, the MC approach leads to a larger asymmetry factor with increasing RH than the SC approach as illustrated in Figs. 1(c) and 1(d). This is a consequence of larger particles being produced more by the MC approach than by the SC approach as the particles grow with increasing RH, but the different rates of water uptake also affect the refractive index of the particles as shown in Eq. (4). Thus this difference in $g$ may be due partly to a smaller rate of growth with increasing RH produced by the SC approach as a result of its use of an effective hygroscopicity for the entire aerosol population. We also note that the difference in $g$ as a result of increased RH between the SC and MC approaches is

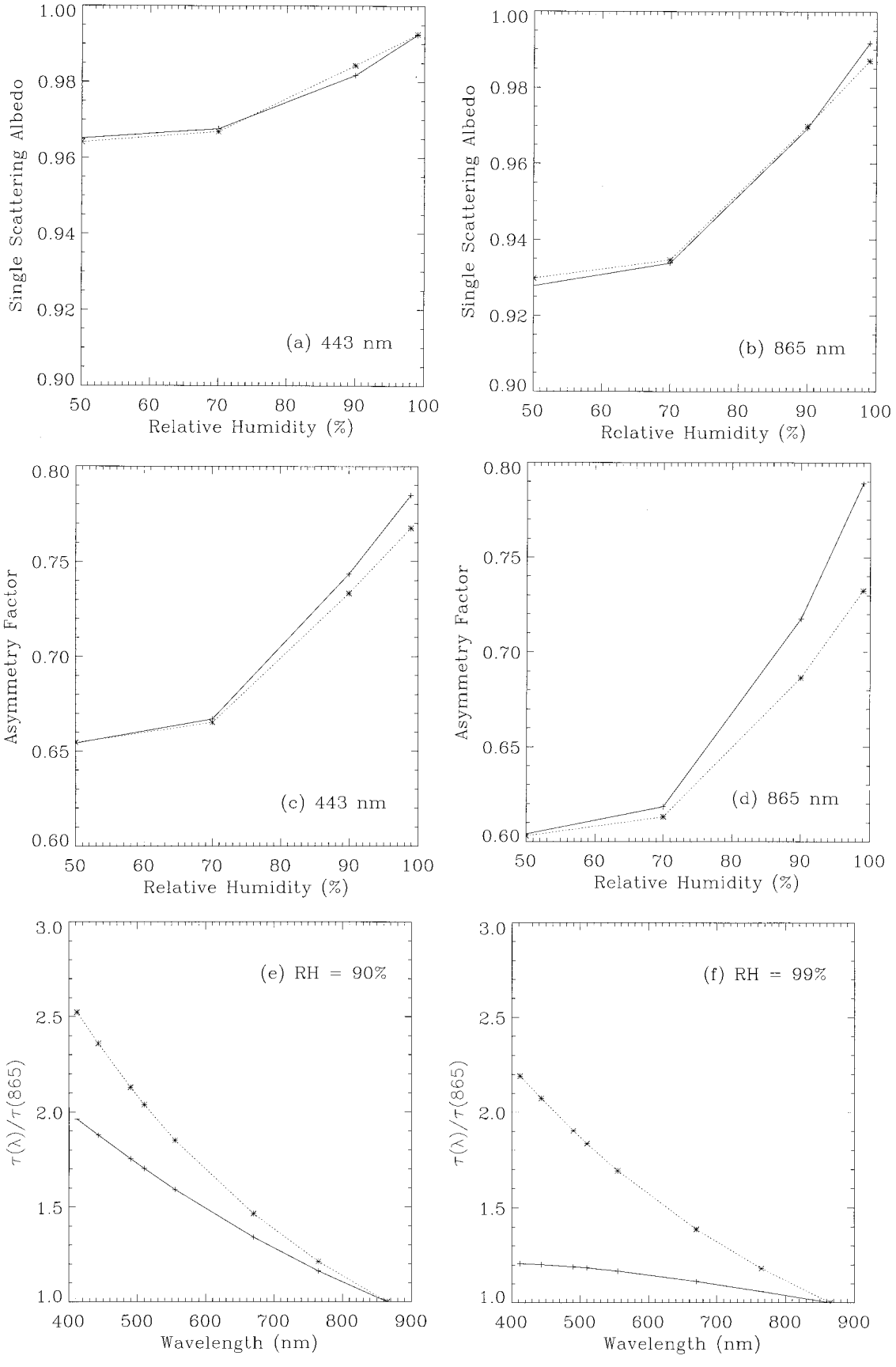


Fig. 1. Comparison of single-scattering albedo SSALB, asymmetry factor $g$, and optical depth $\tau(\lambda)$ for the Tropospheric aerosol model computed with the MC approach (solid curves) and SC approach (dotted curves) at 443 nm and 865 nm. (a) SSALB at 443 nm, (b) SSALB at 865 nm, (c) $g$ at 443 nm, (d) $g$ at 865 nm, (e) $\tau(\lambda)/\tau(865)$ for RH = 90%, and (f) $\tau(\lambda)/\tau(865)$ for RH = 99%.

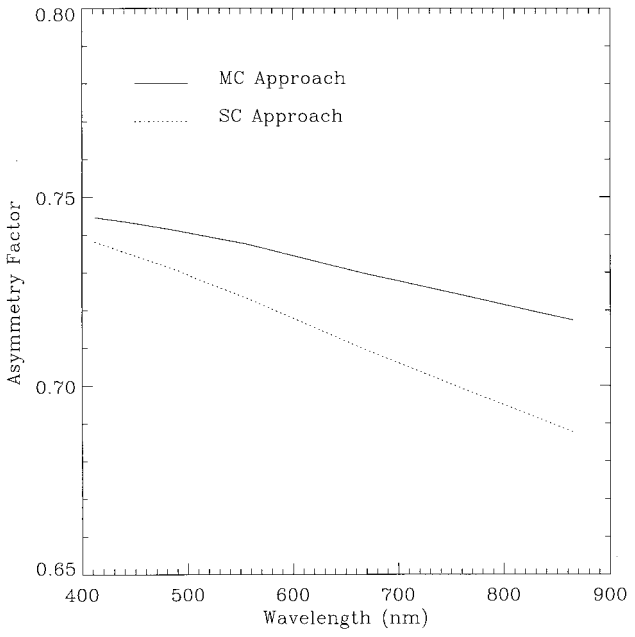


Fig. 2. Comparison of the wavelength dependence of the asymmetry factor obtained with the SC and MC approaches for the Tropospheric aerosol model at RH = 90%.

more pronounced in the NIR spectral region (865 nm) than in the blue region (443 nm).

The SC and MC approaches lead to a spectral dependence of the aerosol optical depth $\tau$ that is markedly different when the RH is high (RH $\geq$ 90%) as shown in Figs. 1(e) and 1(f). Since the dependence of $g$ upon wavelength is stronger in the SC approach than in the MC approach, the spectral dependence of $\tau$ that is obtained with the SC approach is much stronger than that obtained with the MC approach because the spectral dependence of the SSALB is similar in the two approaches. To illustrate this effect, we show in Fig. 2 the dependence of $g$ on wavelength for both the SC and MC approaches at RH = 90%.

Figure 3 shows results similar to those presented in Fig. 1, but for the Urban aerosol model, which contains a mixture of weakly absorbing as well as absorbing aerosols as described above. The results are similar to those obtained in Fig. 1 pertaining to weakly absorbing aerosols, except for the following two points: (i) as shown in Figs. 3(a) and 3(b) the MC approach yields a much higher SSALB than the SC approach except for very high RHs (RH $\geq$ 90%), (ii) as shown in Figs. 3(c) and 3(d) the MC approach yields a smaller $g$ than the SC approach when RH is small (e.g., when RH $\leq$ 90% at 443 nm and when RH $\leq$ 80% at 865 nm).

The Urban aerosol models contain strongly absorbing particles. If the absorbing particles are water soluble or contain a water-soluble coating, then, as the RH increases, the absolute value of the imaginary part of the refractive index of the aerosol is reduced compared to its original value [see Eq. (4)]. When we use the MC approach, this effect is stronger than when we use the SC approach. Thus a larger SSALB is obtained with the MC approach when the RH is smaller than about 95% [see Figs. 3(a) and 3(b)]. The asymmetry factor $g$ is primarily determined by the particle size, but also to some extent by the real part of the refractive index. Thus the larger $g$ values obtained by the SC approach for the relatively dry Urban aerosol model (RH $\sim$ 50%) [see Figs. 3(c) and 3(d)] may be due to the effective refractive index used in this approach. However, as the particles grow with increased RH, the particle size becomes a more important factor in determining $g$. A more comprehensive investigation, beyond the scope of the present study, would be required to explain the detailed behavior of the $g$ values displayed in Figs. 3(c) and 3(d).

## 3. Implications for Atmospheric Correction of Ocean-Color Imagery

Accurate atmospheric correction of ocean-color imagery requires accurate removal of the aerosol contribution to the measured TOA radiance. Errors in the optical properties of the aerosols will directly affect the accuracy of the atmospheric correction. To explore this issue we compare TOA radiances that result from the SC approach with those obtained from the more realistic MC approach. The following results were derived from a radiative-transfer code applicable to the coupled atmosphere–ocean system.[21,22] However, for simplicity we ignored the scattering by particles in the ocean and focused on the aerosol contribution (however, we include scattering by molecules in the air and by density fluctuations in the ocean). Thus in the NIR spectral region the ocean will be "black." For convenience, we define the reflectance $\rho$ as the TOA hemispherical irradiance divided by the extraterrestrial solar irradiance, i.e., $\rho = \pi I/F_0 \cos\theta_0$, where I is the TOA radiance, $F_0$ is the extraterrestrial solar irradiance (normal to the solar beam), and $\theta_0$ is the solar zenith angle. In the following figures we display results for a solar zenith angle of $\theta_0 = 35°$, a polar angle of $\theta = 18°$ and an azimuthal angle of $\phi = 60°$ relative to the solar azimuth.

### A. Top-of-Atmosphere Reflectance Deviation

To compare TOA reflectances that result from the SC approach with those obtained from a more realistic MC approach, we introduce the percentage TOA reflectance deviation defined as

$$\rho_{\mathrm{dev}} = \left[\frac{\rho'_{\mathrm{path}}(\lambda) - \rho_{\mathrm{path}}(\lambda)}{\rho_{\mathrm{path}}(\lambda)}\right] 100\,, \qquad (5)$$

where $\rho'_{\mathrm{path}}(\lambda)$ denotes the total atmospheric contribution to the TOA reflectance obtained with the SC approach, and $\rho_{\mathrm{path}}(\lambda)$ denotes the corresponding contribution obtained with the MC approach.

The vertical distribution of aerosols varies in time and space. In the SeaWiFS algorithm a two-layer model is assumed in the atmosphere: The aerosols occupy the lower layer, and all molecular scattering is

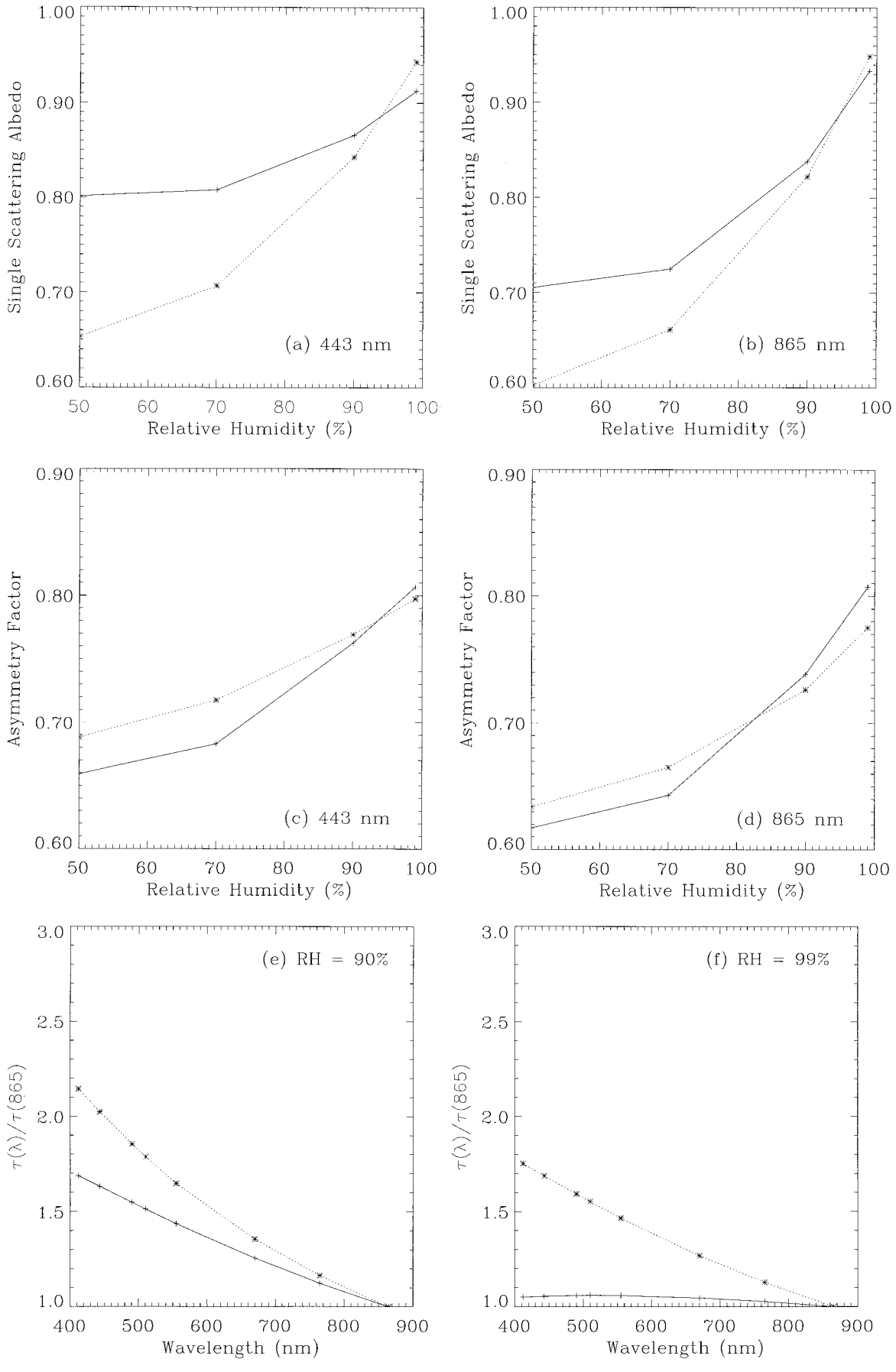


Fig. 3. Similar to Fig. 1 but for Urban aerosols.

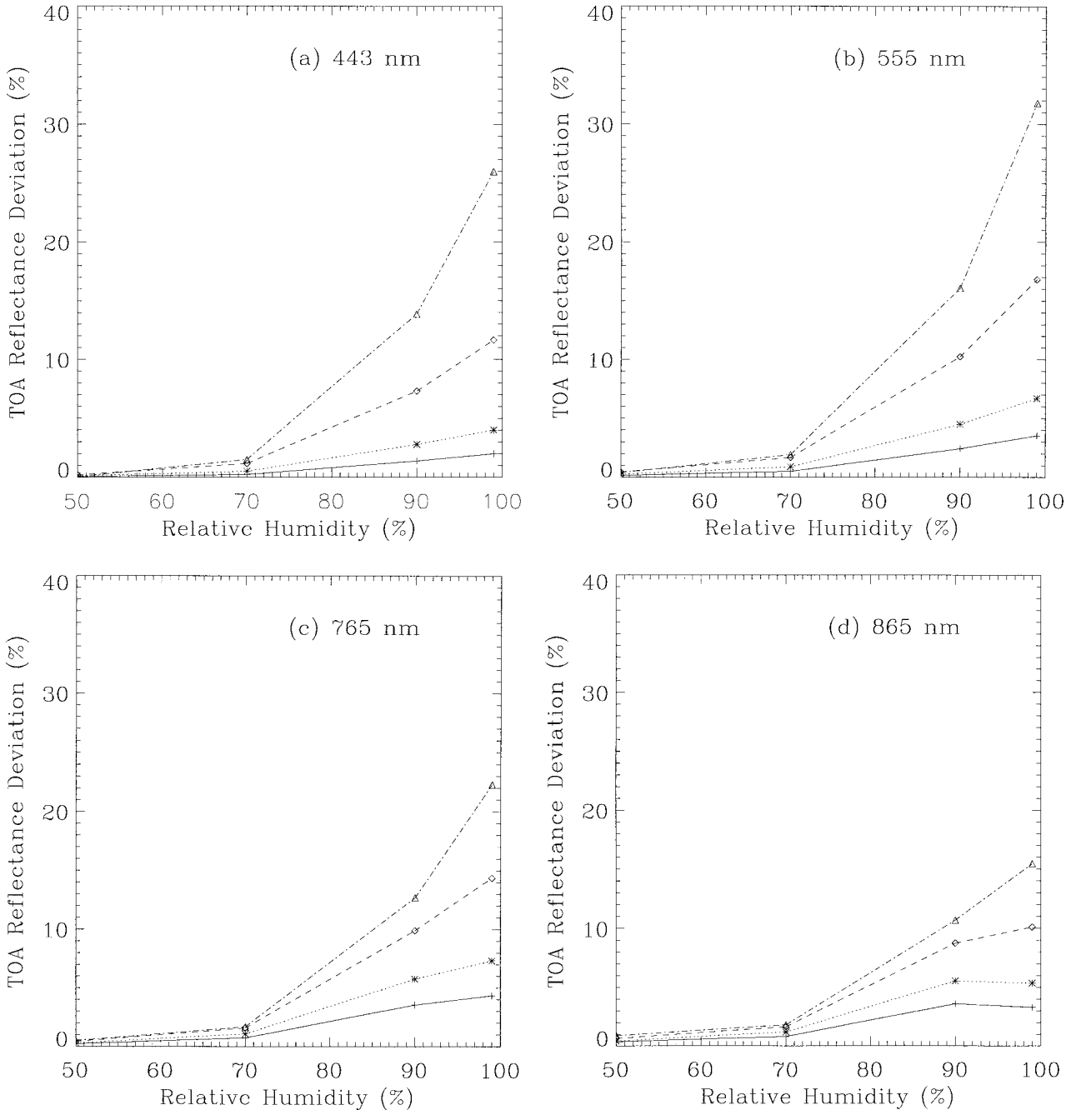


Fig. 4. TOA reflectance deviation defined by Eq. (5) at 443, 555, 765, and 865 nm for the Tropospheric aerosol model. Solid curve, $\tau(865) = 0.05$; dotted curve, $\tau(865) = 0.1$; dashed curve, $\tau(865) = 0.3$; dotted-dashed curve, $\tau(865) = 0.8$.

confined to the upper layer.[4] This distribution of aerosols is similar to that typically found over the oceans when the aerosols are locally generated, i.e., most of the aerosols are confined to the marine boundary layer.[35] Although situations in which a single aerosol layer is confined to the marine boundary layer do occur, there is also evidence for higher layers over the mid-Pacific or Atlantic that result, for example, from dust transport from Asia or the Sahara.[36–39] In marine regions a single aerosol layer is most likely to be composed of sea salt, sulfates, and organics derived from the ocean. Also, the marine boundary layer height is typically 1–2 km.

For demonstration purposes, in the following computations, we allow the aerosols be distributed homogeneously between the surface and 4 km. Although this is unrealistic, it is consistent with the assumptions made in the SeaWiFS atmospheric-correction algorithm. In the comparisons below we select the aerosol optical depth at 865 nm to be the same for the SC and MC approaches. The optical depths at

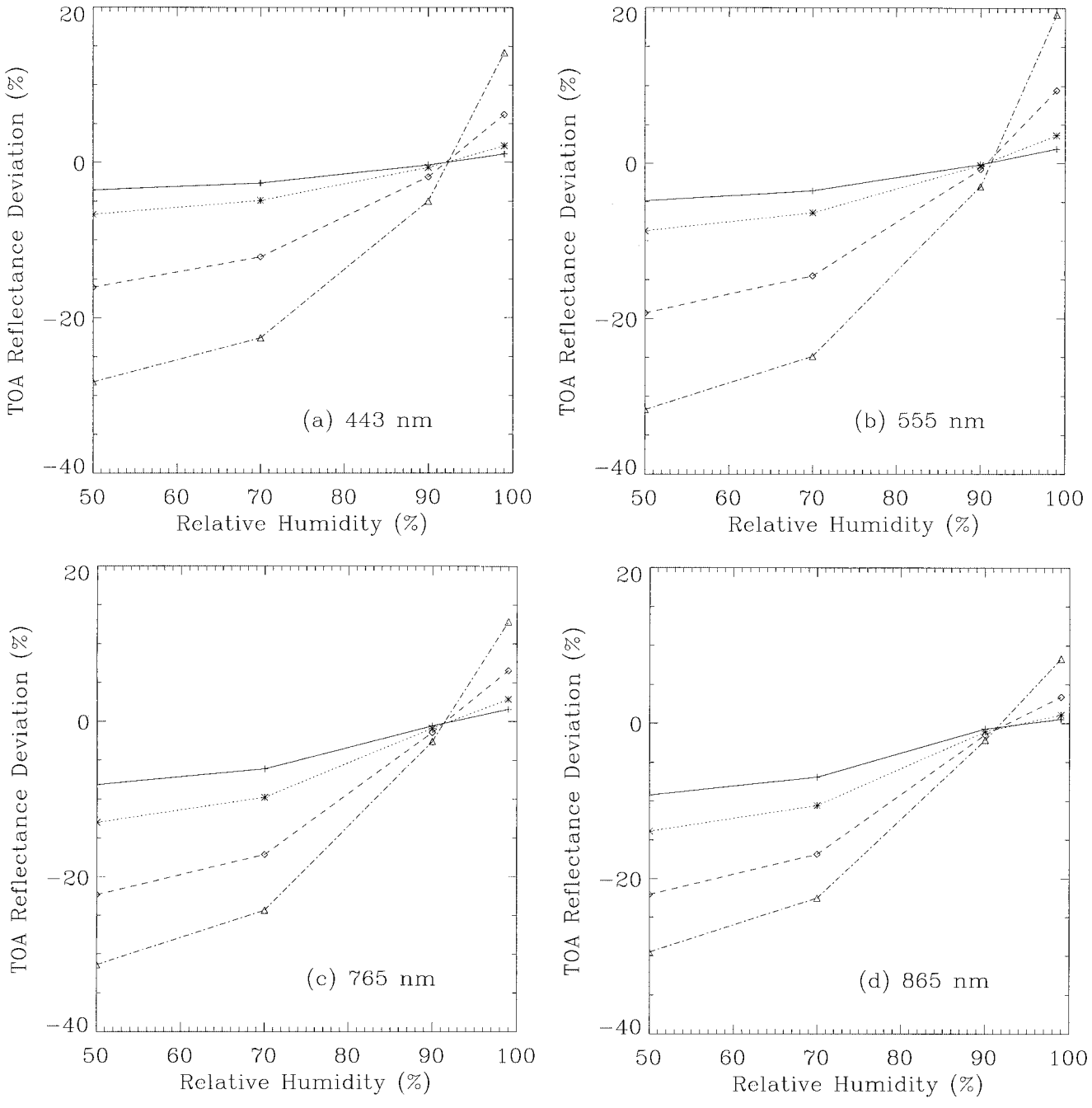


Fig. 5. Same as Fig. 4 but for the Urban aerosol model.

shorter wavelengths will be different for the two approaches as shown in Figs. 1 and 3.

Figures 4 and 5 show the TOA reflectance deviation at four wavelengths for the Tropospheric and Urban aerosol models, respectively. Here the value of the parameter σ defined in Eq. (1) is 0.35 for the Tropospheric aerosol model. The values of σ for the two modes of the Urban aerosol model are 0.35 and 0.4, respectively. The values of $r_i$ ($i$ = 1,2) at several RHs are shown in the Table 1 for these two aerosol models where $r_i$ = 1 and $r_i$ = 2 represent the radii of the two different modes. For the Tropospheric aerosol model, Fig. 4 shows that the smaller asymmetry factor and the larger optical depth obtained with the SC approach lead to an overestimation relative to the MC approach of the TOA reflectance by as much as +32%. Hence, the two approaches lead to significantly different atmospheric corrections. Similar conclusions are obtained for other aerosol models that contain weakly absorbing particles, such as the Coastal and Maritime aerosol models used for atmospheric-correction purposes.

For the Urban aerosol model, Fig. 5 shows that the TOA reflectance deviation changes from being

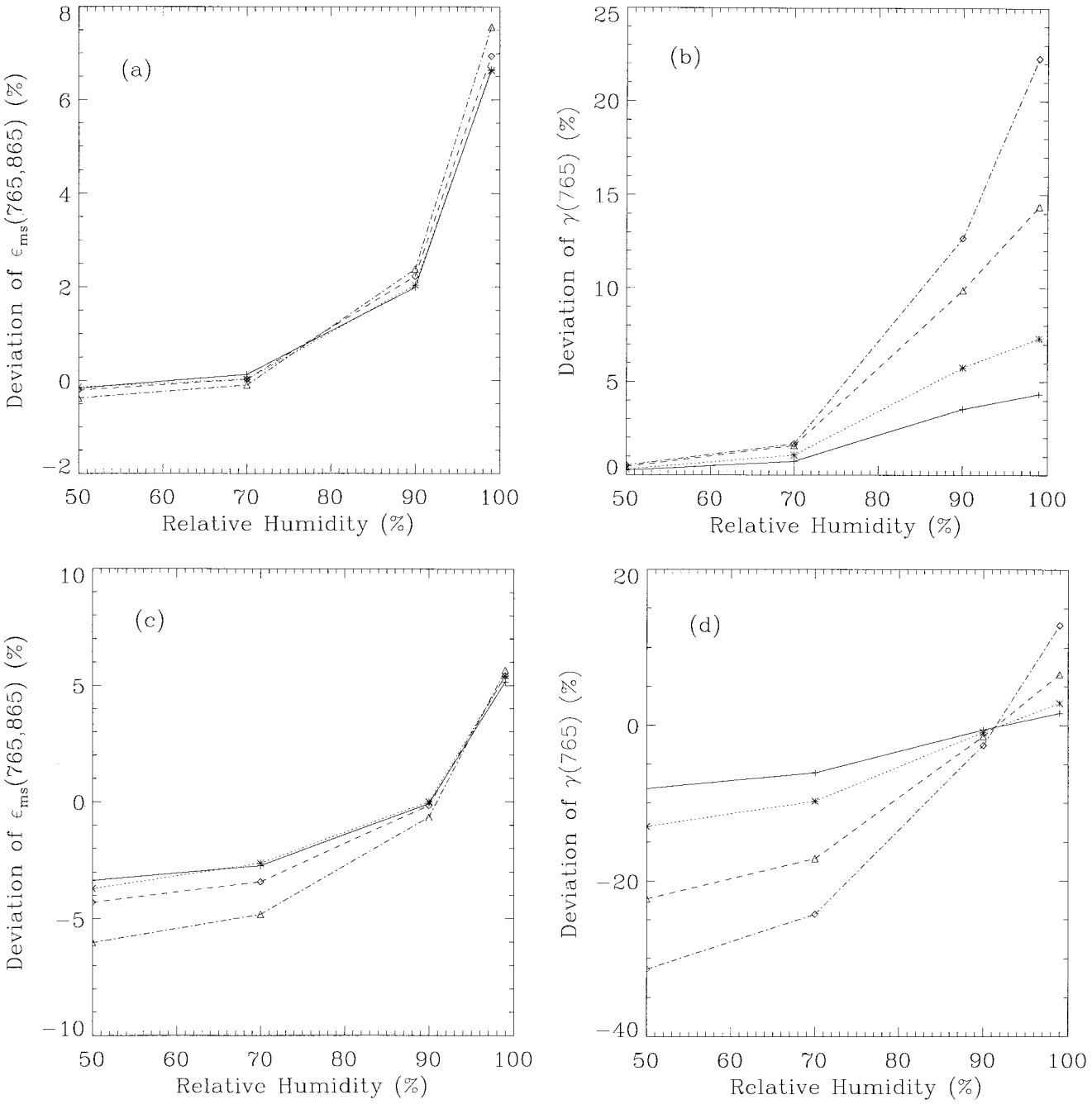


Fig. 6. Deviations of $\epsilon_{ms}(765,865)$ and $\gamma(765)$ computed with the SC approach as compared with the MC approach for several optical depths. Solid curve, $\tau_{865} = 0.05$; dotted curve, $\tau_{865} = 0.1$; dashed curve, $\tau_{865} = 0.3$; dotted-dashed curve, $\tau_{865} = 0.8$. (a) and (b) for the Tropospheric aerosol model; (c) and (d) for the Urban aerosol model.

negative ($-32\%$ at RH = 50%) to becoming positive ($+20\%$ at RH = 99%) as the RH increases. This finding is consistent with the difference in aerosol optical properties that result from the SC approach as compared with the MC approach. This implies that compared with the MC approach the SC approach underestimates the TOA reflectance for low RHs (RH $< 90\%$) and overestimates it when RH $> 90\%$.

Clearly, for both weakly absorbing and strongly absorbing aerosols the SC approach leads to considerable discrepancies in the TOA reflectance relative to the MC approach. In fact, these discrepancies can be as large as or even larger than the contribution by the ocean to the TOA radiance, which is typically a few percent of the total TOA reflectance. Thus these discrepancies are significant and must be accounted for.

### B. $\epsilon_{ms}(\lambda, 865)$ and $\gamma(\lambda)$

The SeaWiFS algorithm for atmospheric correction over case 1 waters employs various ratios, involving the aerosol and the molecular contribution to the

TOA radiance. These ratios are used to select an aerosol model and a corresponding NIR optical depth. On the basis of the selected model the optical depth is then extrapolated from the NIR into the visible, where it is used to quantify the atmospheric contribution to the TOA radiance, so that it can be subtracted from the total. The current operational SeaWiFS algorithm indirectly employs the ratio[4]

$$\epsilon_{ms}(\lambda, 865) = \rho_{ms}(\lambda)/\rho_{ms}(865),$$

where $\rho_{ms}(\lambda) = \rho_{path}(\lambda) - \rho_r(\lambda)$ with $\rho_{path}(\lambda)$ is the total atmospheric contribution and $\rho_r(\lambda)$ is the atmospheric molecular contribution to the TOA (satellite-measured) reflectance. The ratio

$$\gamma(\lambda) = \rho_{path}(\lambda)/\rho_r(\lambda)$$

has been used for atmospheric-correction purposes in the presence of strongly absorbing aerosols.[6]

We show in Figs. 6(a)–6(d) the deviation in both $\epsilon_{ms}$ (765, 865) and $\gamma$ (765) between results obtained with the SC approach and corresponding results that were obtained with the MC approach. In Eq. (5) the deviation is defined as the percentage difference between results obtained with the SC approach as compared to a more realistic MC approach. Figures 6(a) and 6(b) pertain to the Tropospheric aerosol model, while 6(c) and 6(d) pertain to the Urban aerosol model. We note that there is a big difference between $\epsilon_{ms}$ (765,865) and $\gamma$ (765) computed by the SC approach and by a more realistic MC approach. This implies that there will be a difference in the retrieved aerosol optical properties.

## 4. Discussion and Conclusions

Many factors, such as (i) the breakdown of the black-pixel assumption in the NIR spectral region due to algal blooms, air bubbles, or other particles in the ocean, and (ii) insufficient or inadequate aerosol models adopted for atmospheric correction, influence the accuracy of atmospheric correction algorithms and thereby of ocean color retrievals. Each aerosol particle in the atmosphere may consist of a mixture of different chemical components. Thus the computed optical properties of a collection of aerosols will depend on the assumptions we make about how the different components of each particle mix and how each particle grows in size and changes its index of refraction when the relative humidity increases. For the purpose of atmospheric correction of ocean-color imagery, it has been customary to use an effective particle model in which aerosols with different compositions are averaged so as to arrive at a SC aerosol model characterized by a pseudoparticle with an effective refractive index and an effective hygroscopicity. This pseudoparticle is then allowed to grow and change its refractive index as the humidity increases. We have compared this SC approach with a more realistic MC approach in which each aerosol particle keeps its identity (characterized by its original size, hygroscopicity, and refractive index) and is allowed to grow and change its refractive index with increasing humidity, independently of all the other particles. We have used the candidate aerosol models employed in the operational SeaWiFS atmospheric-correction algorithm to assess the consequences of the use of the SC approach instead of a more realistic MC approach in the retrieval process. The results show that there are significant differences in the optical properties (the single-scattering albedo, asymmetry factor and spectral dependence of the aerosol optical depth) obtained with the SC approach as compared with the MC approach. These differences in the optical properties lead to sufficiently large differences in the TOA reflectances that the ocean-color retrieval will be significantly affected. This implies that it becomes important to treat correctly light scattering by aerosols in order to obtain accurate and reliable atmospheric correction and thus be able to retrieve the water-leaving radiance with sufficient accuracy that it can be used to infer chlorophyll concentrations and other marine constituents with known and reasonable accuracy. Retrieval of aerosol chemical and optical properties has received considerable attention in the atmospheric community, owing to the properties' significance in atmospheric chemistry and in climate investigations concerned with the direct and indirect (through clouds) influence of aerosols on the atmospheric radiation balance.[40–42] Correct treatment of aerosol optical properties is of paramount importance in all these investigations. Although the MC approach represents an advancement over the SC approach, there are presently no data available to confirm its accuracy. In view of the limitations of the MC approach that were previously pointed out, a closure experiment to test its validity would be desirable. Such a closure experiment should consist of direct measurements in the marine atmosphere, which include water uptake as a function of aerosol chemical composition, mixing of chemical species within a particle population, and the vertical distribution of aerosols over different ocean regions.

## References


1. C. D. Mobley, "*Light and Water: Radiative Transfer in Natural Waters* (Academic, San Diego, California, 1994).
2. J. T. O. Kirk, *Light and Photosynthesis in Aquatic Ecosystems* (Cambridge U. Press, 1994), 2nd ed.
3. H. R. Gordon and M. Wang, "Retrieval of water-leaving radiance and aerosol optical thickness over the oceans with SeaWiFS: a preliminary algorithm," Appl. Opt. **33,** 443–452 (1994).
4. H. R. Gordon, "Atmospheric correction of ocean color imagery in the Earth Observation System era," J. Geophys. Res. **102,** 17081–17106 (1997).
5. H. R. Gordon, T. Du, and T. Zhang, "Remote sensing of ocean color and aerosol properties: resolving the issue of aerosol absorption," Appl. Opt. **36,** 8670–8684 (1997).
6. D. Antoine and A. Morel, "A multiple scattering algorithm for atmospheric correction of remotely sensing ocean color (MERIS instrument): principle and implementation for atmospheres carrying various aerosols including absorbing ones," Int. J. Remote Sens. **20,** 1875–1916 (1999).
7. M. Schwindling, P. Deschamps, and R. Frouin, "Verification of

aerosol models for satellite ocean color remote sensing," J. Geophys. Res. **103,** 24919–24935 (1998).
8. E. P. Shettle and R. W. Fenn, "*Models for the Aerosols of the Lower Atmosphere and the Effects of Humidity Variations on their Optical Properties* (Air Force Geophysics Laboratory, Hanscomb AFB, Mass., 1979).
9. J. Heintzenberg, "Light scattering parameters of internal and external mixtures of soot and non-absorbing material in atmospheric aerosols," in *Proceedings of the Conference on Carbonaceous Particles in the Atmosphere, Berkeley, Calif., March 20–22, 1978*, T. Novakov, ed. (National Science Foundation/ Lawrence Berkeley Laboratory, Berkeley, Calif., 1978).
10. P. Chylek and J. Wong, "Effect of absorbing aerosol on global radiation budget," Geophys. Res. Lett. **22,** 929–931 (1995).
11. G. Hanel, "The properties of atmospheric aerosol particles as functions of the relative humidity at thermodynamic equilibrium with the surrounding moist air," in *Advances in Geophysics*, H. E. Landsberg and J. Van Mieghem, eds. (Academic, New York) **19,** 73–188 (1976).
12. V. Wulfmeyer and G. Feingold, "On the relationship between relative humidity and particle backscattering coefficient in the marine boundary layer determined with differential absorption lidar," J. Geophys. Res. **105,** 4729–4741 (2000).
13. R. S. Fraser, S. Mattoo, E.-N. Yeh, and C. R. McClain, "Algorithm for atmospheric and glint corrections of satellite measurements of ocean pigment," J. Geophys. Res. **102,** 17107–17118 (1997).
14. B.-C. Gao, M. J. Montes, Z. Ahmad, and C. O. Davis, "Atmospheric correction algorithm for hyperspectral remote sensing of ocean color from space," Appl. Opt. **39,** 887–896 (2000).
15. S.-C. Tsay and G. L. Stephens, *A Physical/Optical Model for Atmospheric Aerosols with Application to Visibility Problems* (Department of Atmospheric Sciences, Colorado State University, Fort Collins, Colo., 1990).
16. G. A. d'Almeida, P. Koepke, and E. P. Shettle, *Atmospheric Aerosols: Global Climatology and Radiative Characteristics* (A. Deepak Publishing, Hampton, Va., 1991).
17. D. M. Murphy, J. R. Anderson, P. K. Quinn, L. M. Mcinnes, F. J. Brechtel, S. M. Kreidenweis, A. M. Middlebrook, M. Posfai, D. S. Thomson, and P. R. Buseck, "Influence of sea-salt on aerosol radiative properties in the southern ocean marine boundary layer," Nature **392,** 62–65 (1998).
18. B. Chen, K. Stamnes, B. Yan, Ø. Frette, and J. J. Stamnes, "Water-leaving radiance in the NIR spectral region and its effects on atmospheric correction of ocean color imagery," J. Adv. Mar. Sci. Tech. Soci. **4,** 329–338 (1998).
19. D. A. Siegel, M. Wang, S. Maritorena, and W. Robinson, "Atmospheric correction of satellite ocean color imagery: the black pixel assumption," Appl. Opt. **39,** 3582–3591 (2000).
20. K. Stamnes, S.-C. Tsay, W. J. Wiscombe, and K. Jayaweera, "Numerically stable algorithm for discrete-ordinate-method radiative transfer in multiple scattering and emitting layered media," Appl. Opt. **27,** 2502–2509 (1988).
21. Z. Jin and K. Stamnes, "Radiative transfer in nonuniformly refracting layered media: atmosphere-ocean system," Appl. Opt. **33,** 431–442 (1994).
22. G. E. Thomas and K. Stamnes, "*Radiative Transfer in the Atmosphere and Ocean* (Cambridge U. Press, New York, 1999).
23. R. W. Fenn, "Aerosol-Verteilungen und atmospharisches Streulicht," Beitr. Physik Atmos. **37,** 69–104 (1964).
24. K. T. Whitby, R. B. Husar, and B. Y. H. Liu, "The aerosol size distribution of Los Angles smog," J. Colloid Sci. **39,** 177–204 (1972).
25. K. T. Whitby, W. E. Clark, V. A. Marple, G. M. Sverdrup, G. J. Sem, K. Willeke, B. Y. H. Liu, and D. Y. H. Pui, "Characterization of California aerosols: I. Size distributions of Freeway aerosol," Atmos. Environ. **9,** 463–482 (1975).
26. K. Willeke, K. T. Whitby, W. E. Clark, and V. A. Marple, "Size distributions of Denver aerosols: A comparison of two sites," Atmos. Environ. **8,** 609–633 (1974).
27. J. T. Twitty, R. J. Parent, J. A. Weinman, and E. W. Eloranta, "Aerosol size distributions: Remote determination from airborne measurements of the solar aureole," Appl. Opt. **15,** 980–989 (1976).
28. F. S. Harris, Jr. and M. P. McCormick, "Mie scattering by three polydispersions," J. Colloid Sci. **39,** 536–545 (1972).
29. C. N. Davies, "Size distribution of atmospheric particles," J. Aerosol Sci. **5,** 293–300 (1974).
30. K. T. Whitby and B. Cantrell, "Atmospheric aerosols—characteristics and measurements," in *The International Conference on Environmental Sensing and Assessment, Las Vegas, Nevada, September 14–19, 1975* (Institute of Electrical and Electronics Engineers, New York, 1975), paper 29-1.
31. G. Hanel and M. Lehmann, "Equilibrium size of aerosol particles and relative humidity: new experimental data from various aerosol types and their treatment for cloud physics application," Contr. Atmos. Phys. **54,** 57–71 (1981).
32. P. V. N. Nair and K. G. Vohra, "Growth of aqueous sulfuric acid droplets as function of relative humidity," J. Aerosol Sci. **6,** 265–271 (1975).
33. E. E. Gard, M. J. Kleeman, D. S. Gross, L. S. Hughes, J. O. Allen, B. D. Morrical, D. P. Fergenson, T. Dienes, M. E. Galli, R. J. Johnson, G. R. Cass, and K. A. Prather, "Direct observation of heterogeneous chemistry in the atmosphere," Science **279,** 1184–1187 (1998).
34. E. Swietlicki, J. Zhou, D. S. Covert, K. Hameri, B. Busch, M. Vakeva, U. Dusek, O. H. Berg, A. Wiedensohler, P. Aalto, J. Makela, B. G. Martinsson, G. Papaspiropoulos, B. Mentes, G. Frank, and F. Stratmann, "Hygroscopic properties of aerosol particles in the north-eastern Atlantic during ACE-2," Tellus B **52,** 201–227 (2000).
35. Y. Sasano and E. V. Browell, "Light scattering characteristics of various aerosol types derived from multiple wavelength lidar observations," Appl. Opt. **28,** 1670–1679 (1989).
36. K. D. Perry, T. A. Cahill, R. A. Eldred, D. D. Dutcher, and T. E. Gill, "Long-range transport of North African dust to the eastern United States," J. Geophys. Res. **102,** 11225–11238 (1997).
37. M. Uematsu, R. A. Duce, J. M. Prospero, L. Chen, J. T. Merrill, and R. L. McDonald, "Transport of mineral aerosol from Asia over the north Pacific ocean," J. Geophys. Res. **88,** 5343–5352 (1983).
38. A. D. Clarke, "Atmospheric nuclei in the Pacific midtroposphere: their nature, concentration, and evolution," J. Geophys. Res. **98,** 20633–20647 (1993).
39. M. Ikemagi, K. Okada, Y. Zaizen, and Y. Makino, "Aerosol particles in the middle troposphere over the northwestern Pacific," J. Met. Soc. Jap. **71,** 517–527 (1993).
40. Y. J. Kaufman, D. Tanre, L. Remer, E. Vermote, A. Chu, and B. N. Holben, "Remote sensing of tropospheric aerosol from EOS-MODIS over the land using dark targets and dynamic aerosol models," J. Geophys. Res. **102,** 17051–17067 (1997).
41. G. K. Yue, J. Lu, V. A. Mohnen, P.-H. Wang, V. K. Saxena, and J. Anderson, "Retrieving aerosol optical properties from moments of the particle size distribution," Geophys. Res. Lett. **24,** 651–654 (1997).
42. I. Chiapello, G. Bergametti, B. Chatenet, F. Dulac, I. Jankowiak, C. Liousse, and E. S. Soares, "Contribution of the different aerosol species to the aerosol mass load and optical depth over the northeastern tropical Atlantic," J. Geophys. Res. **104,** 4025–4035 (1999).